

Arc spot grouping: An entanglement of arc spot cells

Cite as: J. Appl. Phys. **116**, 233302 (2014); <https://doi.org/10.1063/1.4904917>

Submitted: 07 September 2014 . Accepted: 09 December 2014 . Published Online: 19 December 2014

Shin Kajita, Dogyun Hwangbo, Noriyasu Ohno, Mikhail M. Tsventoukh, and Sergey A. Barengolts



View Online



Export Citation



CrossMark

ARTICLES YOU MAY BE INTERESTED IN

[On the mechanism of operation of a cathode spot cell in a vacuum arc](#)

Applied Physics Letters **104**, 184101 (2014); <https://doi.org/10.1063/1.4874628>

[Detailed numerical simulation of cathode spots in vacuum arcs: Interplay of different mechanisms and ejection of droplets](#)

Journal of Applied Physics **122**, 163303 (2017); <https://doi.org/10.1063/1.4995368>

[Plasma parameters of the cathode spot explosive electron emission cell obtained from the model of liquid-metal jet tearing and electrical explosion](#)

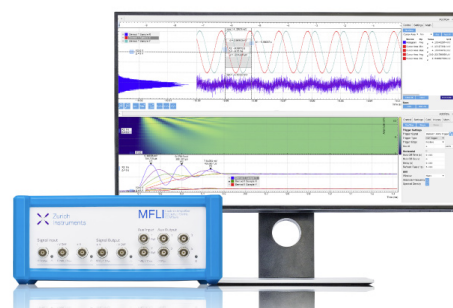
Physics of Plasmas **25**, 053504 (2018); <https://doi.org/10.1063/1.4999377>

Challenge us.

What are your needs for periodic signal detection?



Zurich
Instruments



Arc spot grouping: An entanglement of arc spot cells

Shin Kajita,^{1,a)} Dogyun Hwangbo,² Noriyasu Ohno,² Mikhail M. Tsventoukh,³ and Sergey A. Barenolts⁴

¹*EcoTopia Science Institute, Nagoya University, Nagoya 464-8603, Japan*

²*Graduate School of Engineering, Nagoya University, Nagoya 464-8603, Japan*

³*Lebedev Physical Institute, Russian Academy of Sciences, Moscow 119991, Russia*

⁴*Prokhorov General Physics Institute, Russian Academy of Sciences, Moscow 119991, Russia*

(Received 7 September 2014; accepted 9 December 2014; published online 19 December 2014)

In recent experiments, clear transitions in velocity and trail width of an arc spot initiated on nanostructured tungsten were observed on the boundary of the thick and thin nanostructured layer regions. The velocity of arc spot was significantly decreased on the thick nanostructured region. It was suggested that the grouping decreased the velocity of arc spot. In this study, we try to explain the phenomena using a simple random walk model that has properties of directionality and self-avoidance. And grouping feature was added by installing an attractive force between spot cells with dealing with multi-spots. It was revealed that an entanglement of arc spot cells decreased the spot velocity, and spot cells tend to stamp at the same location many times. © 2014 AIP Publishing LLC. [<http://dx.doi.org/10.1063/1.4904917>]

I. INTRODUCTION

Arcing phenomena are deeply related with various fields of research including high-power circuit interrupter,¹ material deposition of protective coatings and thin films,² switching devices to control electric current flow,³ breakdown phenomena in high-energy accelerators,⁴ and plasma wall interaction in nuclear fusion devices.⁵ Despite of its long history of investigation,^{6,7} there still exist not well-known features in arc spots, e.g., motion of arc spots in magnetic field^{8,9} and grouping of arc spot cells.^{10–12}

Recently, with a usage of nanostructured metal (tungsten), several new features of arcing have been revealed. For example, an unipolar arcing was initiated in a controlled way in laboratory plasma devices,^{13–15} magnetic field dependence of self-affine fractality has been clearly identified,¹⁶ and grouping feature of arcing was observed on the arc trail.¹⁷ The advantage of the usage of the nanostructured medium is likely to be in the changes in some physical properties. An increase of the field electron emission current and a decrease of the thermal conductivity¹⁸ make it easier to initiate arcing, and by a significant change in the optical reflectance, trail can be clearly recorded on the surface containing a clear footprint of arc spot.

In recent experiments, clear transitions in velocity and trail width were observed on the boundary of the thick and thin nanostructure layer.¹⁹ The velocity of arc spot was significantly decreased on the thick nanostructured region, suggesting that the formation of grouping decreased the velocity of arc spot. The experimental results exhibited interesting and essential characteristics in grouping feature of arc spot cells. Earlier, we attempted to interpret the experimental results by considering the processes occurring during the operation of an individual cell of the cathode spot of a vacuum arc^{19,20} in the context of the explosive-emission center (ecton) model of a

cathode spot.²¹ It has been shown that as a spot cell moves to a thick nanostructured layer, the size of the crater it leaves increases and its velocity decreases. However, these parameters also depend on the unknown current carried by the cell. Also, the model used gives no way to consider possible grouping of cells in an individual cathode spot and the complicated trajectory of motion of the spot observed in experiments. Grouping of spot cells is possible due to favorable conditions of their operation in the immediate vicinity to each other.¹² As the cell current and the exact number of cells in a spot are unknown, we here consider the motion of such “grouped” cathode spots.

In this study, we try to explain the phenomena using a random walk model. Previously, the motion of arc spots on the nanostructured tungsten was modeled with a random walk model that has directionality, self-avoidance, and bifurcation features.¹⁶ In this study, by expanding the model, grouping feature is installed. It will be shown from the simulation that an entanglement of spot cells alters the global motion of arc spots significantly and provides possible explanation for the experimental observation. In Sec. II, after a brief summary of the experiments using special configuration with a sample having two different nanostructured thickness regions, the random walk model used in this study is described. In Sec. III, results and discussion are provided, and conclusions are given in Sec. IV.

II. PREPARATIONS

A. Essence of experiments

Here, a brief review of the previous experiment and detailed scanning electron microscope (SEM) analysis of the samples are given. Arcing experiments were conducted in the linear plasma device NAGDIS-II. Figure 1(a) shows a schematic of the experimental setup. A stationary plasma was produced using a discharge gas of helium at the pressure of several mTorr by dc arc discharge. An LaB₆ disk heated

^{a)}Electronic mail: kajita.shin@nagoya-u.jp

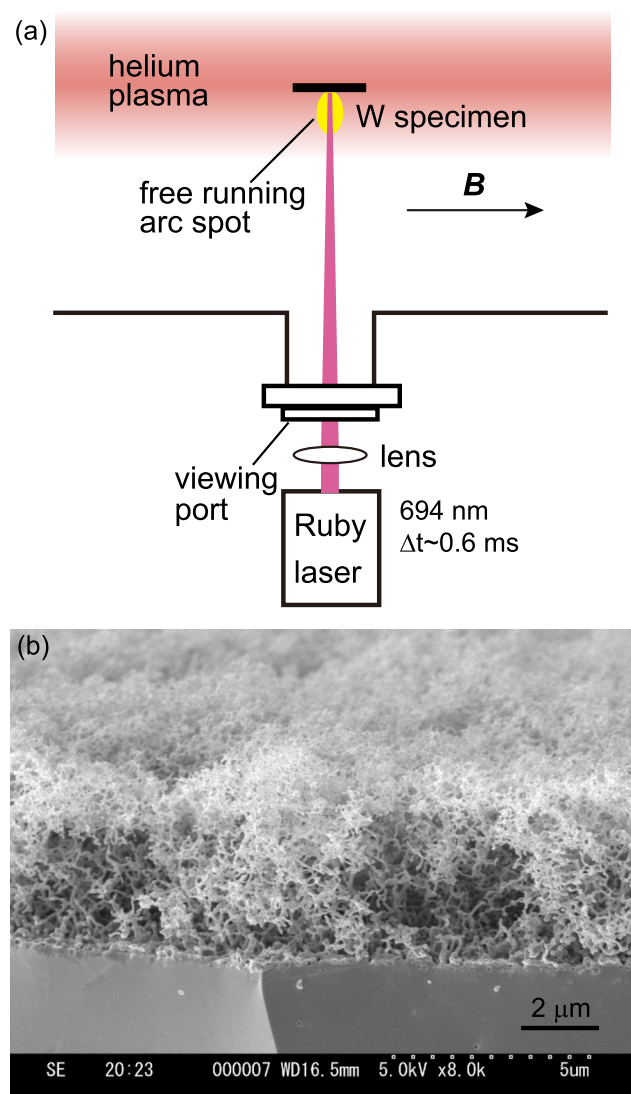


FIG. 1. (a) A schematic of the experimental setup and (b) an SEM micrograph of He irradiated W sample.

from the backside with a carbon filament is used for cathode, and a DC arc discharge produces plasmas in steady state. Along with the magnetic field line with the strength of 0.05 T formed by solenoidal coils, the helium plasma produced in the source region was diffused to the downstream. The plasma production region was approximately 1.5 m away from the position where an arcing electrode was installed. The typical electron density and temperature of the stationary plasma are 10^{19} m^{-3} and 5 eV, respectively, in the downstream region. The arcing is initiated on the tungsten electrode positioned in the downstream region. From recent spectroscopic measurement results, the density and temperature of unipolar arc spot initiated on tungsten are likely to be approximately 10^{20} and 0.5–0.7 eV, respectively.²² To trigger the arcing, a pulsed laser irradiated the sample, while the sample was negatively biased by an electric power supply. Although it is possible to trigger arcing even when the target is at the floating potential (the case corresponds to unipolar arcing), the target was negatively biased from external to make it easier to trigger arcing in this study. An arc spot was produced from the laser irradiated position, and it freely runs

on the surface in the retrograde, i.e., $-\mathbf{j} \times \mathbf{B}$, direction. It is interesting to note that the electrode is surrounded by the stationary plasma when the arcing is initiated, and a current loop is formed through the plasma. In the present study, the arc current was limited by the power supply and was $\sim 4 \text{ A}$.

Another unique point addressed about the experiments is the morphology of the electrode. Figure 1(b) shows a cross sectional SEM micrograph of the electrode. When tungsten is exposed to the helium plasma, nanostructures were formed on the surface.²³ The helium plasma irradiation leads to the formation of nanosized helium bubbles near the surface, and the growth of the helium bubbles leads to the formation of nanostructures. The width of the fiberform structure is approximately 20–30 nm. The thickness of the nanostructured layer can be controlled by the helium fluence to the surface. The formation of the nanostructures makes it easier to initiate arcing in response to pulsed heat loads, probably because of an increase in the field emission current density and a decrease in the thermal conductivity. To observe the influence of the layer thickness on the arcing behavior, we covered half of the sample when the sample was exposed to the helium plasma. The sample used in the experiments had two regions with different helium fluences. The initiated arc spots were observed with a fast framing camera and the arc trail was observed by SEM after the experiment.

Figure 2(a) shows the SEM micrograph of the arc trail around the boundary between thick and thin nanostructured layer parts. The thickness of the nanostructured layer was approximately $4 \mu\text{m}$ at the thick nanostructure layer region and $1 \mu\text{m}$ at the thin nanostructure layer region. Hereafter, the two regions are called thick and thin regions, respectively. It is seen that the width of the trail on the thick region was significantly wider than that on the thin region.

Figure 2(b) shows the distributions of the trail width in the thick and thin regions. On the thin region, the width is typically several tens of micrometer, while it has a broad distribution from 200 to $600 \mu\text{m}$ in the thick region. Trail width was deduced from the widest part of the trail, i.e., maximum consecutive black pixels in vertical direction in Fig. 2(a). Figures 2(c) and 2(d) show the average trail width and velocity, respectively, on the thin and thick regions. The velocity was deduced from the fast framing camera observation of the arc spots. The trail width became wider on the thick region by a factor of 8, and the spot velocity decreased by a factor of 7.

Figures 3(a) and 3(b) show the SEM micrographs of the arc trail on the thin region. Trail basically moves in a form of a single spot. On the arc trail, since the amount of the electron emission decreased, the brightness of the SEM images decreased. On the arc trail, there are many black dots representing pinholes on the surface even after the arc spot destroyed the fine structures. Figures 4(a) and 4(b) show the SEM micrographs of the arc trail on the thick region. The inside structure can be observed from the SEM micrographs. On the thick region, the trail was formed by a congregation of smaller spot traces; it shows the grouping feature of the spot same as the trail shown in Ref. 17. The wider trail is composed of smaller arc trails with the width of $\sim 10 \mu\text{m}$. Moreover, as seen in Fig. 4(a), difference in the contrast can

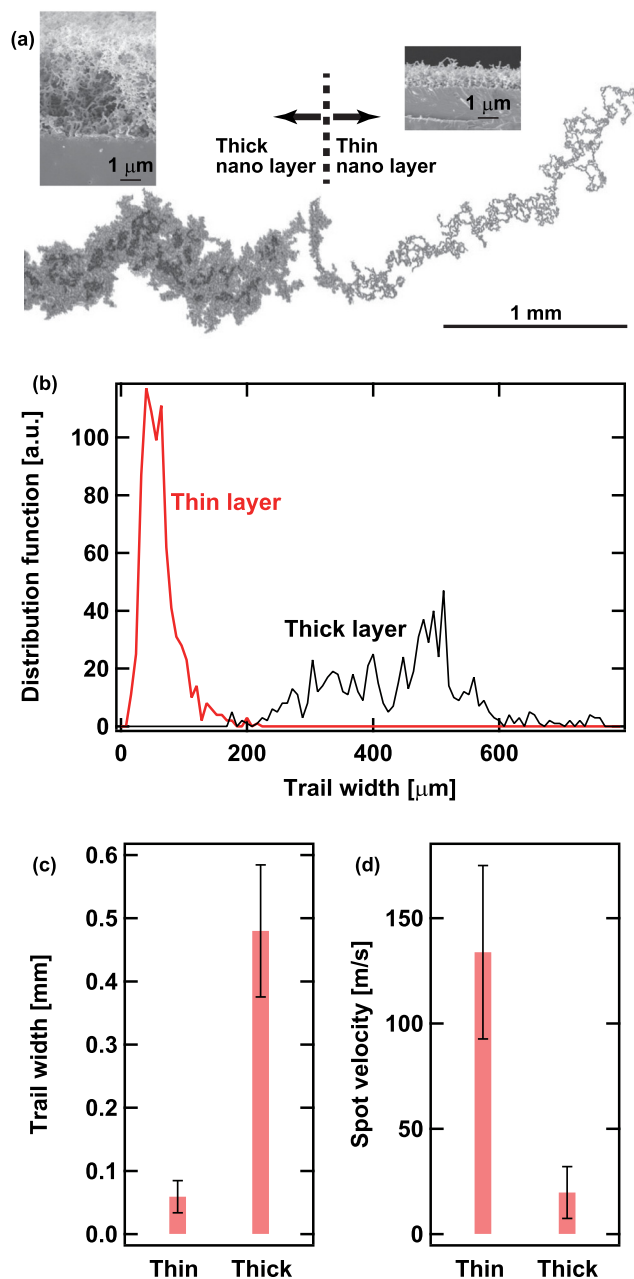


FIG. 2. (a) Arc trail recorded on the nanostructured W, (b) distributions of the trail width, (c) the averaged trail width, and (d) the averaged spot velocity on the thick and thin nanostructured layer.

be identified even inside the trail, indicating that the surface morphology is different by location. In some parts, the surface totally melted, while other part has droplets on fine structures. Since the melted part would have lower electron emission, the SEM image became darker. On the location where melting is significant, pinholes cannot be identified on the surface.

B. Model

Since arc spot motion is essentially viewed as a random walk, a Monte Carlo simulation has been used to explain the motion. Previously, to explain the motion of spot cell on nanostructured tungsten, a random walk model that includes

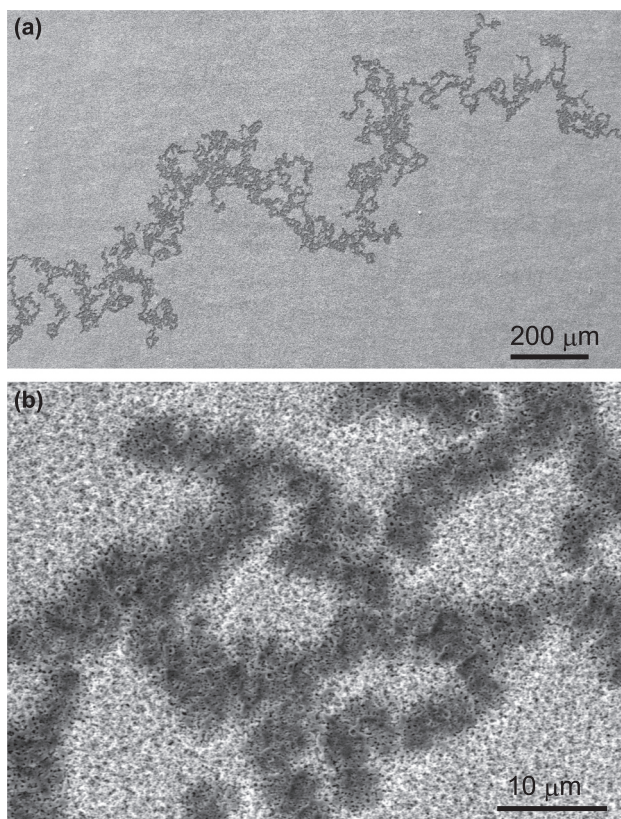


FIG. 3. SEM micrographs of the arc trail on the thin region.

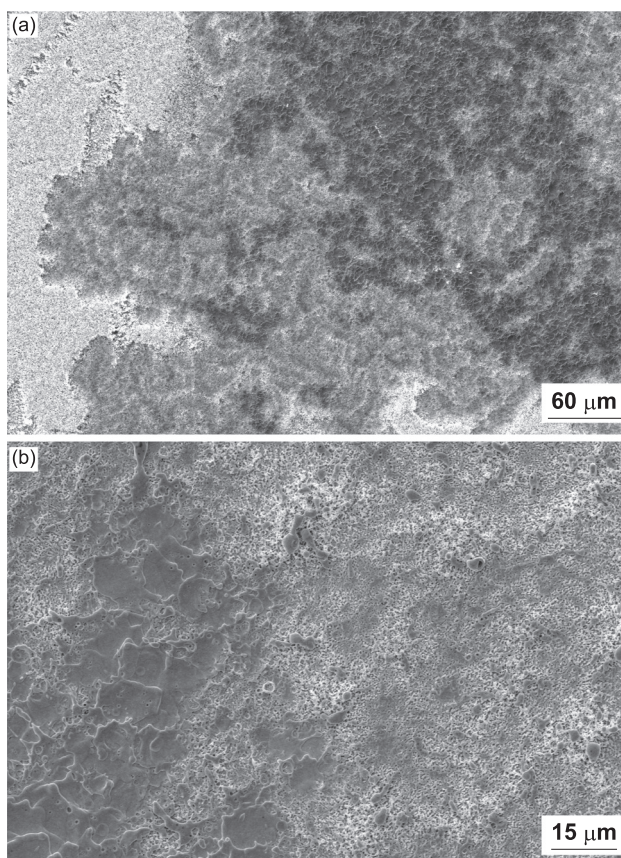


FIG. 4. SEM micrographs of the arc trail on the thick region.

directionality, self-avoiding effect, and bifurcation was developed.¹⁶ Figure 5(a) shows a schematic illustrating a two dimensional random walk model. The location of the spot cell is represented as a black colored cell. The cell can move in adjacent four cells, namely, $+x$, $-x$, $+y$, and $-y$ directions. In a normal random walk model, the spot cell moves in the four directions at same probability. Here, to quantitatively discuss the probability, relative probabilities to move the four directions are introduced as R_{+x} , R_{-x} , R_{+y} , and R_{-y} , respectively. The actual probability to $+x$ direction, for example, is written as

$$P_{+x} = \frac{R_{+x}}{R_{+x} + R_{-x} + R_{+y} + R_{-y}}. \quad (1)$$

When the cell has directionality, the probability to the direction was increased.

Figure 5(b) illustrates 3×3 cells with the number of stamping, N_{st} . In the left figure, the spot cell is in the left in the center cell, and the number of stamping in all the other cell is zero. When it moves to the center cell, the number of stamping in the center cell becomes one. Because the

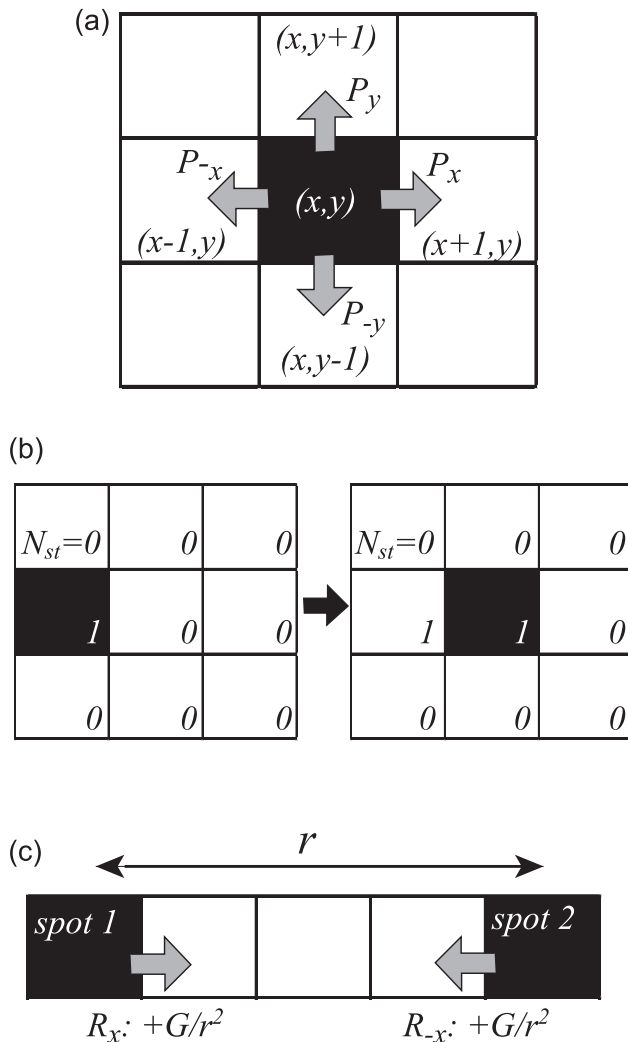


FIG. 5. Schematics for explaining the model of spot motion. (a)–(c) are for explaining the probability of the motion of a spot cell, attractive force between spots, and the number of stamp times, respectively.

nanostructures are destroyed by arcing and it makes it difficult to initiate arcing at the same location, self-avoiding effect is taken into account. For a complete self-avoiding random walk model, spot cell cannot move to the location where $N_{st} > 0$. In reality, however, since it is likely that arcing can reignite also on the location where nanostructures were destroyed, we decreased the relative probability to move the location, rather than to use a complete self-avoiding model. Also, split of cell has been observed in experiments, and in the previous model, to introduce the phenomena to the random walk model, probabilities of bifurcation and extinction of a cell were defined.

In this study, to introduce grouping feature, multi-spot model with attractive force between spot cells is introduced without extinction and bifurcation of cells. Directionality was introduced by increasing the probability to move $+x$ direction. The relation between the field strength and the increase in the probability for directionality was discussed in Ref. 24; the increase in the probability was $\sim 7.5\%$ when the magnetic field strength was 0.05 T. Considering the fact that the probability can be varied by the influence of the bifurcation, etc., we simply increase R_{+x} by 10%.

Usually, if there are wires with the electric current in the same direction, they attract each other. However, for arc spots, it is not so simple to explain the attractive force. For example, an arc spot moves retrograde ($-\mathbf{j} \times \mathbf{B}$) direction. Various mechanisms are proposed to explain the phenomena. At the moment, it is likely that magnetic pressure formed with the combination of the arc spot current and external field may play a role to move that direction.²⁵ In that sense, the spot cells do not attract each other, in the same manner as their retrograde motion. It is likely that a decrease in the magnetic pressure between arc spot cells takes place, and it acts as a repulsive force, not an attractive force. We can specify a repulsion force that is proportional to $1/r$, where r is the distance between the two cells, since the retrograde velocity v_{retr} is proportional to the external magnetic field strength B ,²⁶ and B decreases with r as $B \propto I/r$, where I is the cell current.

On the other hand, from the observation of arc spot and trails, apparent attraction takes place between spot cells as well, if we take into account that the motion of spot is essentially not the motion of the spot as a whole but ignition and death of its cells. The ignition probability is increased by the overlap of the plasmas, the density of which decreases with the distance from the spot center. Roughly, it can be assumed that the probability increases with the density, n_e and $n_e \propto 1/r^2$. The choice of this relation was dictated by that the probability of initiation of a new ecton during the interaction of the cathode plasma with the cathode surface is substantially determined by the plasma density^{27–29} and that the plasma expansion from the cathode spot region is nearly spherically symmetric.³⁰ Here, we assume that the new cathode spot cell is initiated by the interaction of the erosion plasma with the surface of the electrode in contrast to Refs. 31 and 32, where the possibility of thermal instability of the metallic surface at the interaction with the ambient plasma was examined. Erosive plasma density is much higher, which leads to an increase in emission current³¹ and

transition to explosive electron emission. Assuming that two spots have the same plasma density, the attractive force satisfies the following relation:

$$F_{\text{att}} \propto \frac{1}{r^2}. \tag{2}$$

When the number of the spot cell, N_{sp} , is more than two, the attractive force for the i th arc cell can be written as

$$F_{\text{att}}^i \propto - \sum_{j \neq i} \frac{1}{|r_{ij}|^2} \frac{r_{ij}}{|r_{ij}|}, \tag{3}$$

where r_{ij} is the vector of which the direction is from the i th to j th cell with the magnitude of the distance between the two spot cells. To include this force in the model, the probability to move the direction should be increased in proportion to the force presented in Eq. (3). For that purpose, a coefficient G is installed to connect the force in Eq. (3) and an increase in the probability.

Figure 5(c) shows a schematic illustrating the attractive force between cells. When the attractive force is introduced, the relative probability toward a cell is increased by

$$- \sum_{j \neq i} \frac{G}{|r_{ij}|^2} \frac{r_{ij}}{|r_{ij}|}, \tag{4}$$

where G is the attractive force coefficient and the number of cell is used instead of using the real distance. An increase in G results in the increase of the probability of the initiation of cells closed to each other and consequently the increase the spot cell density. Therefore, conceptually, the parameter G represents the level of grouping properties of cathode spot.

Concerning self-avoiding effect, it was introduced by decreasing probability to move to the location where $N_{st} > 0$ by a factor of 10. In the model, collisions between the spot cells were avoided. When another spot cell exists at the adjacent cell, the movement to the direction is prohibited. When the spot cell number increased, the movable direction of a spot cell could be decreased if other cells surrounded it.

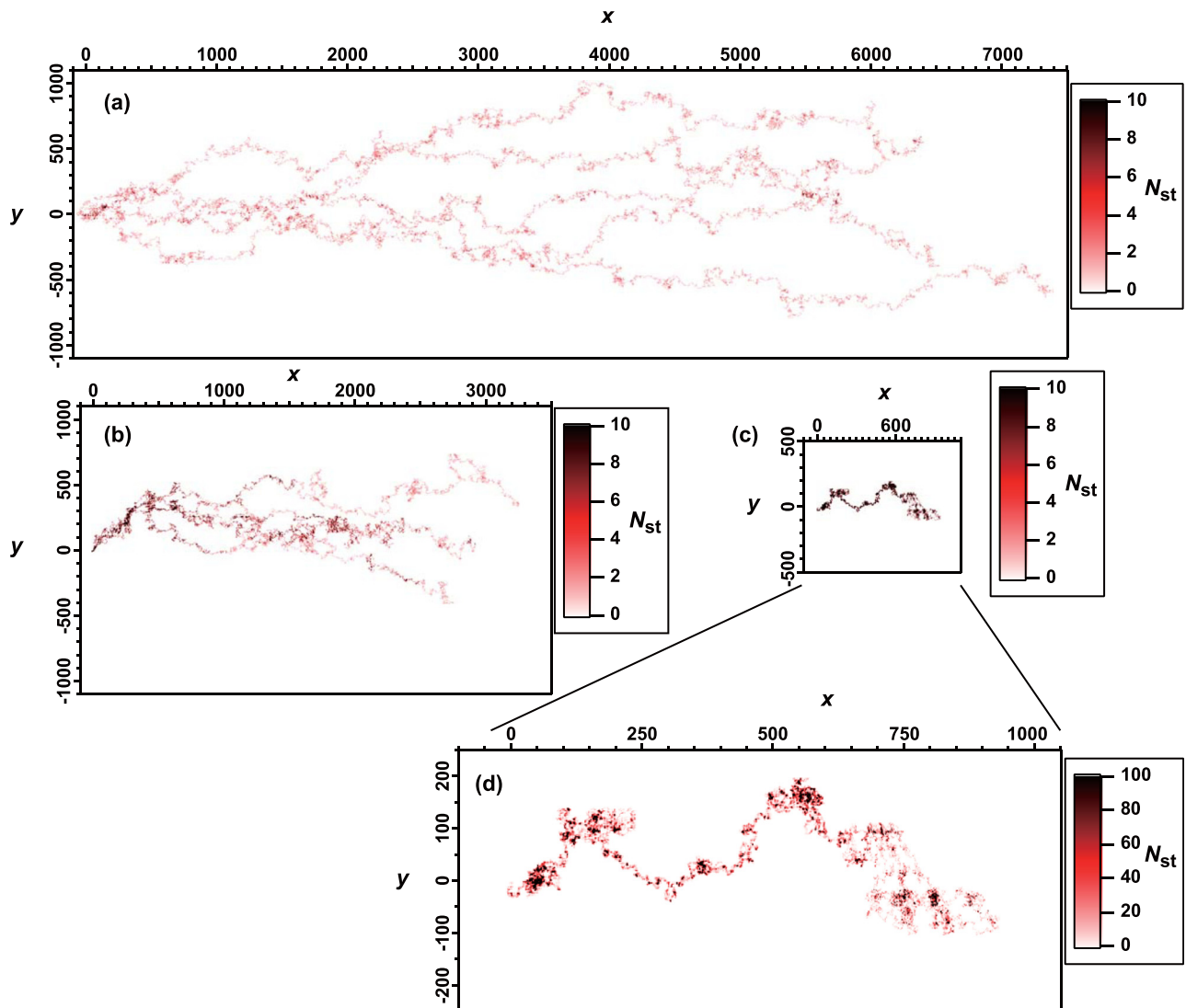


FIG. 6. Calculated trails of random spots. The attractive force coefficient was (a) $G = 30$, (b) $G = 100$, and (c) $G = 200$. The spot number is five and the number of steps was 200 000 for each spot.

III. RESULTS AND DISCUSSION

Figure 6 shows some typical calculated trails for the number of spot cells, N_{sp} , of five with the number of step of 200 000. The attractive force coefficient G in Figs. 6(a)–6(c) was 30, 100, and 200, respectively. When $G=30$, spot moves almost randomly without any strong interaction between spot cells. When $G=100$, the trail length decreased to less than half that at $G=30$, though the spot cells seem to move randomly. When $G=200$, all the five spot cells were entangled together, and a darker line with N_{st} was formed. Enlarged trail for $G=200$ is shown in Fig. 6(d), in which the maximum contrast corresponds to one order higher N_{st} of 100. On the trail, N_{st} is basically less than ten; it is greater than 100 in some places.

It is identified that spots cells entangled with each other and form grouping when increasing the attractive force between spot cells. In the following part, the features of the trail are investigated with changing the attractive force and the number of spot cells from the perspective of the velocity and width of the grouped arc spots and N_{st} , and discussion is given with a comparison to the experimental results.

A. Velocity and width

Figure 7(a) shows the trail length in x direction as a function of G for different N_{sp} , i.e., 3, 5, and 10, after the run of 200 000 steps. The trail length significantly decreased with increasing G . It seems that there is a threshold in G to form grouping, and the threshold increases with N_{sp} . When $N_{sp}=3$, the length started to decrease from $G=10$, while

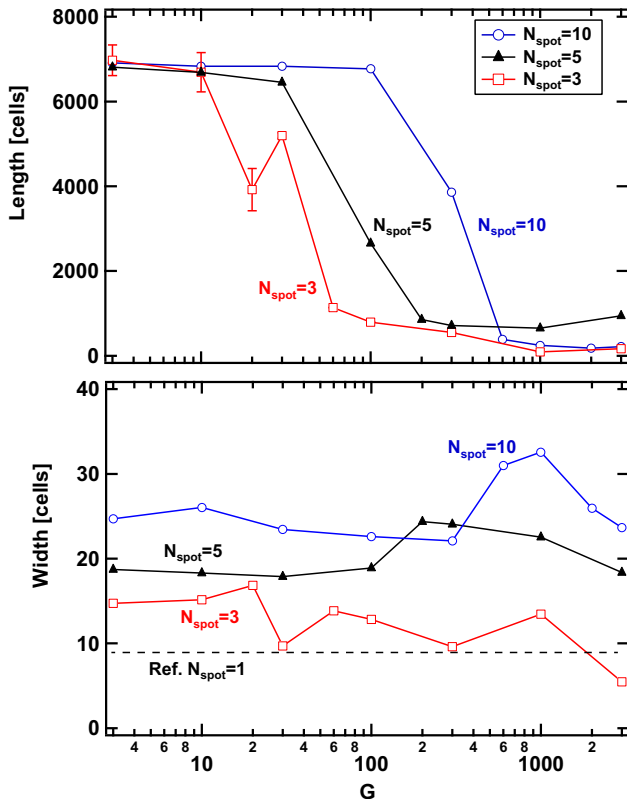


FIG. 7. (a) Trail length and (b) width of the trail as a function of G for different spot numbers.

the length did not change until $G=100$ for $N_{sp}=10$. In the random walk simulation, assuming that the time of a step, i.e., re-ignition time, is not altered even when N_{sp} increases, the decrease in the length corresponds to the decrease in the velocity. Thus, the result exhibits that an entanglement of spot cells occurs and decreases the global velocity of the spot when the attractive force exceeds some level, which increases with the number of spot cells. In experiments, the trail velocity was decreased by a factor of 8. In Fig. 7, the length shortened roughly by an order of magnitude when G was sufficiently greater for all N_{sp} .

Figure 7(b) shows the trail width as a function of G . Trail width was deduced from the widest part of the trail and averaged over the whole trail, the same as in Fig. 2(b). When $N_{sp}=1$, the average width was ~ 9 , as indicated with a dotted line in Fig. 7(b). Although the trail width increased with increasing N_{sp} , it did not have a clear dependence on G . In other words, in the present model, the width of the trail does not change even when spot cells entangle and form a group, though it can be increased when N_{sp} is increased. For $N_{sp}=5$ and 10, the averaged width was increased to 20–25 and 25–32, respectively; the width increased up to a factor of 3.5. The reasons to cause the discrepancy between the experiments and simulation will be discussed later.

B. Increase in the number of stamping

Figure 8 shows the number of cells where arc spots are formed as a function of N_{st} for $G=30, 100,$ and 200 for $N_{sp}=5$. From Fig. 7(a), transition occurred from $G=30$ to 200, and the trail length decreased from 6500 to less than 1000. Spot cells did not entangle at all at $G=30$, while they completely grouped at $G=200$. The profiles of the number of spot cells significantly altered before and after the formation of grouping. Without grouping, it has a steep profile with a short tail. On the other hand, the distribution became flatter with a tail at greater N_{st} with increasing G .

Figure 9 shows the averaged N_{st} as a function of G for $N_{sp}=3, 5,$ and 10. Without grouping, the averaged N_{st} was

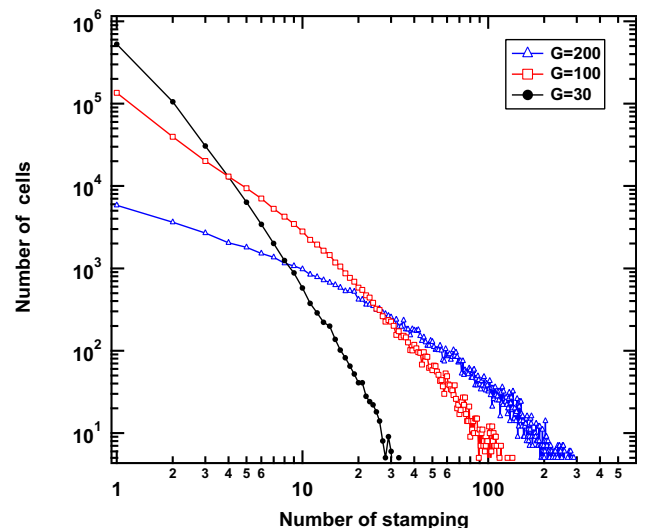


FIG. 8. The number of cells as a function of N_{st} for $G=30, 100,$ and 200 in the case of $N_{sp}=5$.

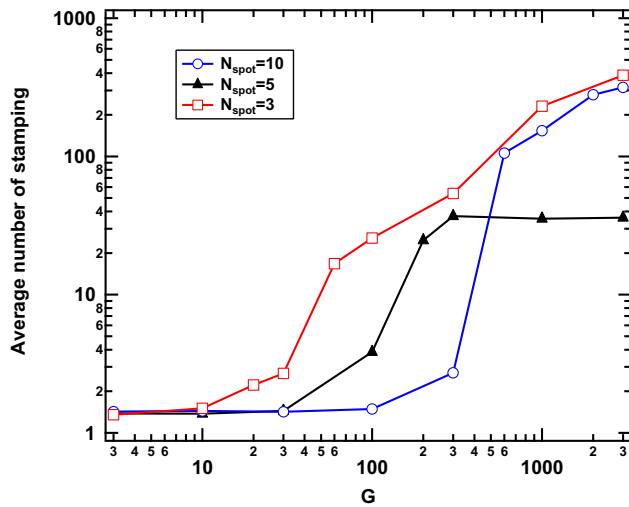


FIG. 9. The averaged N_{st} as a function of G for $N_{sp} = 3, 5$, and 10 .

less than two. However, it significantly increased when the grouping was formed. When $N_{sp} = 5$, the averaged N_{st} saturated at ~ 30 , while it continuously increased with G when $N_{sp} = 3$ and 10 and is greater than 100 .

When G is small, i.e., here $G = 30$, and the attractive force is not large enough to change the motion of spot cells around, spot cells hardly move to locations where $N_{st} > 0$, meaning that they behave in a self-avoiding manner. On the other hand, when the attractive force becomes large enough to change the motion of the spot cells around, the attractive force dominates the self-avoiding effect and spot cells can move to locations where $N_{sp} > 0$.

C. Discussion

By the introduction of the attractive force, an entanglement of spot cells was realized. It was shown that the entanglement can decrease the spot velocity and increase N_{st} . Physically, this is because the entanglement of spot cells decreases the influence of directionality and self-avoiding effect. In other words, the grouping can increase the number of re-stamping at a place and decrease the velocity. In experiments, at the trail of grouped spots, nanostructured layer was totally eliminated, though single spot can remain some of the nanostructured part. This may be caused by the increase in the number of stamping. Also, from the simulation, it was shown that the increase in N_{sp} increases the width of the trail. Here, a comparison is made between the simulation results and experimental observation.

Considering the fact that the velocity decreased by a factor of 7 in experiments, the corresponding G in the simulation is ~ 100 for $N_{spot} = 3$, > 200 for $N_{spot} = 5$, and ~ 500 for $N_{spot} = 10$, from Fig. 6(a). That is, when attractive force is large enough and entanglement occurs, the reduction ratio of the global spot velocity in the simulation is consistent with that observed in the experiments. With increasing N_{sp} , greater attractive force is required to form the entanglement. This is partly because the attractive force from various directions can cancel out each other and some spots can be released from the entanglement. At the corresponding G

values, i.e., $G \sim 100$ for $N_{spot} = 3$, $G > 200$ for $N_{spot} = 5$, and $G \sim 500$ for $N_{spot} = 10$, the averaged N_{st} is almost the same at 30–50 even when the number of spots is different. This indicates that the number of stamping can be an order of magnitude greater when spot entanglement takes place under the present experimental condition. In the experiments, the thick nanostructures were fully destroyed and the layer was eliminated totally. The thickness of the eroded layer can be an order of magnitude greater on the thick region. It may be caused by the fact that the re-ignition of spot cells occurs at the same locations more than ten times due to the formation of the spot entanglement.

Our calculations have suggested that the principal cause of the decrease in velocity of a cathode spot as it arrives at a thick nanostructured layer is an increase in parameter G . As noted above, increasing the parameter G increases the cell density in the cathode spot. When the cells become closer to each other, the spot trajectory becomes more intricate and the velocity of its directional motion as a whole decreases. The reason for this is that as a cell is lost, a new one can arise only in a place free from other cells, which can occur most probably either at the edge of the spot or in the region where the spot cells were already operated. This is due to that the operation of a cell several times in one place of a nanostructured layer destroys the layer incompletely, as distinct from the thin region. The proposed model is supported by experimental data on the motion of a cathode spot on a thin-film cathode with variable film thickness in an external magnetic field, as seen in Ref. 35. In Ref. 35, a single cathode spot consisting of several cells operated in the region with a larger film thickness (high G , see Fig. 6(c)), while it disintegrated into a number of independent spots when the spot came in the region with a smaller film thickness (low G , see Fig. 6).

On the arc trail in the thick region, nanostructures were totally disappeared and molten traces remained on the surface, as seen in Fig. 4. The melting and vaporization of the nanostructured layer were caused by the processes that the spot operated several times on one place in the thick region. This led to intense surface heating of the bulk cathode and formation of a molten-metal pool, promoting for re-ignition of the spot cells.^{33,34} In Fig. 4, we can see overlapping of spot trails, which is characteristic of second-type spots operating on clean metal surfaces.^{7,34} When an arc operates on a nanostructured surface, the probability of initiation of new cathode spots depends not only on the cathode plasma density but also on the geometry of individual nanofibers. In this case, the operation of the arc is similar in many respects to that of an arc with first-type cathode spots spaced some distance from each other, moving, however, randomly and directionally (in the tangential magnetic field), with substantially higher velocities. In this connection, the increase in parameter G on arrival of cathode spots at a thick nanostructured layer can be accounted for by that they start behaving like second-type spots, when nanostructured layer is totally destroyed.

Concerning the width, Fig. 7(b) indicated that the greater number of spot cells is necessary to explain the enhancement of the width by a factor of 8. The width of the

trail of a cathode spot can also depend on the spot cell size. In the foregoing, we supposed that the spot cell size is the same for thick and thin regions. Also, the discrepancy might be caused by the fact that the present model does not well simulate the actual spot motion in some parts. One possibility is in the widening of the trail by a spot split, which was not included in this study. In the previous study, the bifurcation increases the fractal dimension of the trail,¹⁶ suggesting that it can also increase the width. Also, in the present study, extinction of the spot was not included. Bifurcation and extinction, which should occur in the actual situation, change the N_{st} and width. Other possibility is in the modeling of self-avoiding effects. Although the re-ignition probability was decreased by a factor of 10 when $N_{st} > 0$ in the calculation, it might decrease with N_{st} in actual situation and the reduction in the re-ignition probability could be much greater than ten if N_{st} is higher. In this study, even if the spot cell was surrounded by the cells where $N_{st} \geq 10$, it should move somewhere; in the actual situation, the spot could extinct, and another new spot might appear by bifurcation at the point where $N_{st} = 0$. If those effects could be introduced to the model, the width of the trail could be increased several times and be closer to experimental results. It is expected that those detailed investigations will be conducted in future with further experimental evidences.

IV. CONCLUSIONS

In this study, a grouping feature of arc spots, which can significantly alter the spot velocity and erosion rate of electrode materials, was modeled with using a random walk simulation. This study provided an insight of spot grouping phenomena assuming that an attractive force acts between spot cells. This investigation was initiated from the experimental observation recently reported,¹⁹ in which arc spot motions were investigated on a tungsten sample with nanostructures formed by helium plasma irradiation. The sample had two regions: one part had 1 μm thick nanostructure layer (thick region), while the other part had 4 μm thick nanostructure layer (thin region). The spot cells form grouping on the thick region, while single spot cell moves randomly on the thin region. From the first framing camera observation, the spot velocity decreased on the thick region by a factor of 7. And the trail width recorded on the sample increased on the thick region by a factor of 8. From the SEM observation, the nanostructures were totally destructed on the thick region. On the other hand, on the thin region, some fine structures still remained even after the arc spot destroyed the structures.

To model the grouping feature of arc spot cells, an attractive force was introduced to a random walk model based on Monte Carlo method, assuming that the density profile, i.e., ignition probability, had a profile with $1/r^2$ dependence, where r is the distance between two spot cells. It is demonstrated that an entanglement of spot cells occurs and spot cells moves together with forming a group when the attractive force between spot cells is sufficiently strong. When the entanglement takes place, the spot velocity significantly decreased and the number of stamping times

significantly increased. Without entanglement, the self-avoiding effects, i.e., spot cells does not move to the locations where cathode spot was initiated before, and directionality, i.e., spot cells tend to move in some direction, well appeared in the simulation results. However, when spot cells entangle each other, the attractive force between spot cells dominates the self-avoiding effects and directionality. Consequently, the spot velocity decreases and the spot can move to locations where arc spot had been initiated. When the velocity decreased by a factor of 7, the number of stamping times can be roughly 30–50 times. The increase in the number of stamping times can be one of the reasons to enhance the erosion and significant destruction of nanostructures on the thick region. The width of the trail can increase with the size and the number of the spots.

The experimental and simulation results would provide important perspective for grouping phenomena. In nuclear fusion devices, the database about the erosion rate of material by arcing would be necessary to predict the material lifetime, and the grouping feature significantly changes the erosion rate. Because the nanostructures are possibly formed on the material surface on the plasma facing components, the present experiments directly correspond to the situation. For the future study, it will be of importance to observe the level of grouping under various conditions and material experimentally and investigate the physics behind the attractive force with the help of theoretical and simulation studies.

ACKNOWLEDGMENTS

This work was supported in part by a Grant-in-Aid for Young Scientists (A) 23686133 from the Japan Society for the Promotion of Science (JSPS). This work was also supported in part by NIFS/NINS under the project of Formation of International Scientific Base and Network and by RFBR Grant No. 14-08-01137.

- ¹Vacuum Arcs, *Theory and Application* (Wiley, New York, 1980), p. 120.
- ²R. L. Boxman and V. N. Zhitomirsky, *Rev. Sci. Instrum.* **77**, 021101 (2006).
- ³R. L. Boxman, S. Goldsmith, and A. Greenwood, *IEEE Trans. Plasma Sci.* **25**, 1174 (1997).
- ⁴Z. Insepov, J. Norem, A. Moretti, D. Huang, S. Mahalingam, and S. Veitzer, e-print [arXiv:1003.1736v4](https://arxiv.org/abs/1003.1736v4).
- ⁵R. Behrisch, *Physics of Plasma-Wall Interactions in Controlled Fusion*, Nato ASI Series, Series B, Physics (Plenum Pub. Corp., 1986), pp. 495–513.
- ⁶B. Jüttner, V. F. Puchkarev, E. Hantzche, and I. Beilis, *Handbook of Vacuum Arc Science and Technology* (Noyes Publications, 1995), pp. 73–264.
- ⁷A. Anders, *Cathodic Arcs: From Fractal Spots to Energetic Condensation* (Springer, New York, 2008).
- ⁸I. Beilis, *IEEE Trans. Plasma Sci.* **30**, 2124 (2002).
- ⁹K. C. Lee, *Phys. Rev. Lett.* **99**, 065003 (2007).
- ¹⁰B. E. Djakov and R. Holmes, *J. Phys. D: Appl. Phys.* **7**, 569 (1974).
- ¹¹I. Beilis, B. E. Djakov, B. Jüttner, and H. Porsch, *J. Phys. D: Appl. Phys.* **30**, 119 (1997).
- ¹²G. Mesyats and S. Barengolts, *IEEE Trans. Plasma Sci.* **29**, 704 (2001).
- ¹³S. Kajita, S. Takamura, and N. Ohno, *Nucl. Fusion* **49**, 032002 (2009).
- ¹⁴D. Nishijima, Y. Kikuchi, M. Nakatsuka, M. Baldwin, R. Doerner, M. Nagata, and Y. Ueda, *Fusion Sci. Technol.* **60**, 1447 (2011).
- ¹⁵D. Aussems, D. Nishijima, C. Brandt, H. van der Meiden, M. Vilemova, J. Matejicek, G. D. Temmerman, R. Doerner, and N. L. Cardozo, *J. Nucl. Mater.* (in press).

- ¹⁶S. Kajita, N. Ohno, Y. Tsuji, H. Tanaka, and S. Takamura, *J. Phys. Soc. Jpn.* **79**, 054501 (2010).
- ¹⁷S. Kajita, N. Ohno, S. Takamura, and Y. Tsuji, *Phys. Lett. A* **373**, 4273 (2009).
- ¹⁸E. Dechaumphai, J. L. Barton, J. R. Tesmer, J. Moon, Y. Wang, G. R. Tynan, R. P. Doerner, and R. Chen, *J. Nucl. Mater.* **455**, 56 (2014).
- ¹⁹D. Hwangbo, S. Kajita, S. A. Barengolts, M. M. Tsventoukh, and N. Ohno, *Results Phys.* **4**, 33 (2014).
- ²⁰S. Barengolts, G. Mesyats, and M. Tsventoukh, *Nucl. Fusion* **50**, 125004 (2010).
- ²¹G. Mesyats, *IEEE Trans. Plasma Sci.* **23**, 879 (1995).
- ²²D. U. Aussems, D. Nishijima, C. Brandt, R. P. Doerner, and N. J. Cardozo, *J. Appl. Phys.* **116**, 063301 (2014).
- ²³S. Takamura, N. Ohno, D. Nishijima, and S. Kajita, *Plasma Fusion Res.* **1**, 051 (2006).
- ²⁴S. Kajita, S. Takamura, and N. Ohno, *Plasma Phys. Controlled Fusion* **53**, 074002 (2011).
- ²⁵B. Jüttner, *J. Phys. D: Appl. Phys.* **34**, R103 (2001).
- ²⁶K. Zabello, Y. Barinov, A. Chaly, A. Logatchev, and S. Shkol'nik, *IEEE Trans. Plasma Sci.* **33**, 1553 (2005).
- ²⁷G. Mesyats and D. Proskurovsky, *Pulsed Electrical Discharge in Vacuum* (Springer-Verlag, 1989).
- ²⁸I. V. Uimanov, *IEEE Trans. Plasma Sci.* **31**, 822 (2003).
- ²⁹D. Shmelev and S. Barengolts, *IEEE Trans. Plasma Sci.* **41**, 1964 (2013).
- ³⁰S. Barengolts, G. Mesyats, and D. Shmelev, *J. Exp. Theor. Phys.* **93**, 1065 (2001).
- ³¹A. Nedospasov and V. Petrov, *Dokl. Akad. Nauk SSSR* **269**, 603 (1983) (in Russian).
- ³²A. Nedospasov and B. Shelukhaev, *Dokl. Akad. Nauk SSSR* **295**, 102 (1987) (in Russian).
- ³³G. A. Mesyats and N. M. Zubarev, *J. Appl. Phys.* **113**, 203301 (2013).
- ³⁴G. Mesyats, M. Bochkarev, A. Petrov, and S. Barengolts, *Appl. Phys. Lett.* **104**, 184101 (2014).
- ³⁵I. G. Kesaev, *Cathode Processes in Electric Arc* (Moscow, 1968), Fig. 60, p. 137 (in Russian).